

International Journal of Modern Physics A
 © World Scientific Publishing Company

LORENTZ VIOLATION IN THREE-FAMILY NEUTRINO OSCILLATION

SHIMIN YANG

*School of Physics and State Key Laboratory of Nuclear Physics and Technology,
 Peking University, Beijing, 100871, China*

BO-QIANG MA

*School of Physics and State Key Laboratory of Nuclear Physics and Technology,
 Peking University, Beijing, 100871, China
 mabq@phy.pku.edu.cn*

Received Day Month Year

Revised Day Month Year

We analyze the consequences of Lorentz violation (LV) to three-generation neutrino oscillation in the massless neutrino sector. We present a general formalism of three-family neutrino oscillation with neutrino flavor states being mixing states of energy eigenstates. It is also found that the mixing parts could strongly depend on neutrino energy by special choices of Lorentz violation parameters. By confronting with the existing experimental data on neutrino oscillation, the upper bounds on LV parameters are derived. Because the oscillation amplitude could vary with the neutrino energy, neutrino experiments with energy dependence may test and constrain the Lorentz violation scenario for neutrino oscillation.

Keywords: Lorentz violation; Neutrino mass and mixing; Neutrino oscillation.

PACS numbers: 11.30.Cp, 12.15.Ff, 13.15.+g, 14.60.Pq

1. Introduction

Lorentz invariance has been a fundamental principle in physics since Einstein established special relativity in 1905. In the last century, numerous experiments provided precise verifications of Lorentz invariance, and most current data are consistent with this symmetry. Over the last decade there is a growing interest in studying Lorentz invariance violation in the physics society. Though no theoretical model predicts Lorentz violation conclusively, there have been some theoretical suggestions that Lorentz invariance may not be an exact symmetry at all energies. In particular, many works to describe the force of gravity within the context of a quantum theory imply the breaking of Lorentz symmetry (including string theory^{1,2}, warped brane worlds³, and loop quantum gravity⁴). Other high energy models of space structure could also contain Lorentz violation⁵. Even if Lorentz symmetry is broken at high energy, there can still be an attractive infrared fixed point⁶. So we can still get an

approximate Lorentz invariant world at low energy range. Besides above theoretical motivations, many other models, such as emergent gauge bosons^{7,8}, varying moduli⁹, ghost condensate¹⁰, space-time varying coupling^{11,12}, or varying speed of light cosmology^{13,14} also incorporate Lorentz violation. Whether Lorentz symmetry is perfectly unbroken under all conditions is still an important theoretical question.

Lorentz invariance violation was proposed as a solution to two important experimental problems, i.e., the observation of TeV photons and of cosmic ray events above the GZK cutoff^{15,16,17,18,19}, for a review see Ref. 20. In the first case, it is hard to observed ultrahigh energy photons coming from ulterior galaxies since cosmic gamma rays with energy above 10 TeV should interact with cosmic infrared background photons and convert into electron-positron pairs. However, the High Energy Gamma Ray Astronomy (HEGRA) satellite detected 24 TeV gamma rays from Markarian 501²¹. In the second case, ultra high energy cosmic rays interact with cosmic microwave background photons and produce pions. The cosmic rays lose energy through this process until they pass below the GZK cutoff energy 10^{19} eV^{22,23}. However, there has been report that the cosmic ray spectrum extends beyond this energy²⁴. Lorentz violation could give a preparative solution to the two problems because the threshold energy at which the cutoff occurs could be altered by modifying special relativity, though it is not the only way to explain these problems. We also aware²⁵ that recent HiRes²⁶ and Pierre Auger²⁷ measurements of the ultrahigh energy cosmic rays show a sharp suppression around the energy of 10^{19} eV, which is consistent with the expected cutoff energy. If the phenomenon of GZK cutoff is confirmed by further experiments, Lorentz invariance will still be a good symmetry in the area of ultra high energy cosmic ray. Therefore one would need to look at other possibilities for the breakdown of Lorentz invariance.

Neutrinos provide another interesting laboratory for studying the possibility of Lorentz violation. If Lorentz invariance is violated by quantum gravity, the natural scale one would expect a strong Lorentz violation is the Planck energy of 10^{19} GeV²⁸. But the attainable energy of accelerator is of TeV scale. So it is difficult to directly detect Planck scale Lorentz violation in the laboratory. However, there might be a small amount of Lorentz violation at lower energies if Lorentz symmetry is violated at Planck scale. Neutrinos offer a promising possibility to study Lorentz violation that may exist at the low-energy as the remnants of Planck-scale Physics²⁹. Neutrino oscillation is an important problem in neutrino physics. To explain this kind of phenomena, the conventional scenario is to assume that neutrinos have masses. In this assumption, there is a spectrum of three or more neutrino mass eigenstates and the flavor state is the mixing state of mass eigenstates^{30,31}. Coleman and Glashow pointed out that neutrino oscillation can take place even for massless neutrinos if Lorentz invariance is violated in the neutrino sector³². In Ref. 16, they assumed that the maximum attainable speed of a particle depends on its identity and that the flavor states are the mixing states of speed eigenstates, and analyzed neutrino oscillation quantitatively. In Ref. 33 a two-generation model

to study neutrino oscillations is established. This model involves a mass term and a single nonzero coefficient for Lorentz violation. Kostelecký and Mewes presented a general formalism for violations of Lorentz and CPT symmetry in three-family massive neutrino oscillation³⁴. In their calculation the mixing part has the same form comparing with that of the conventional massive neutrino scenario because of their assumption that neutrinos are massive. They also built a special model called bicycle model in massless neutrino sector³⁵, in which the Lorentz violation parameters are direction-dependent. Ref. 36 built a three-neutrino massive model with Lorentz-violating terms. All classes of neutrino data are described in this model, including LSND oscillation data. Grossman *et al.* studied the interactions between the neutrino and the Goldstone boson of spontaneous Lorentz violation, and proposed a novel dynamic effect of Goldstone-Čerkev radiation, where neutrinos moving with respect to a preferred rest frame can spontaneously emit Goldstone bosons³⁷. Arias *et al.* analyzed the consequences of Lorentz violation in the massless neutrino sector by deforming the canonical anti-commutation relations for the fields³⁸. Morgan *et al.* analyzed atmospheric neutrino oscillations at high energy by modified dispersion relations and placed bounds on the magnitude of this type of Lorentz invariance violation³⁹.

In this paper, we study Lorentz violation contribution to neutrino oscillation. In our calculation we assume that neutrinos are massless and that the neutrino flavor states are mixing states of energy eigenstates. We calculate neutrino oscillation probabilities by the effective theory for Lorentz violation, which is usually called the standard model extension (SME)^{40,41}. In our work, the mixing angles for neutrinos are functions of Lorentz violation parameters.

The structure of this paper is as follows. In Sect. 2, we figure out the neutrino oscillation probabilities by the effective theory for Lorentz violation. In Sect. 3, we introduce some specific models and give the numerical values for LV parameters by comparing our theoretical oscillation probabilities with experimental results. Then we analyze the dependence of the new oscillation equation on neutrino energy and neutrino propagation length. Remarks and conclusions are given in Sect. 4.

2. Theoretical framework for Lorentz violation and neutrino oscillation probabilities

In the conventional massive neutrinos scenario, neutrino mass eigenstates are components of neutrino flavor states. Neutrinos change from one flavor to another during the propagation, because the phase of time for each mass eigenstate is different. However, Lorentz invariance violation may be another origin for neutrino oscillation. In this work, we analyze the consequences of Lorentz violation in the massless neutrino sector. Different from the conventional massive neutrino model, neutrino flavor states are mixing states of eigenenergy in our calculation. The bounds on LV parameters will be given by comparing our calculation with the experimental results. In this part we will figure out the neutrino oscillation probability. The

4 *Shimin Yang and Bo-Qiang Ma*

general and detailed calculation method for neutrino oscillation was proposed in Ref. 34. However, for the integrity of the article, we display the entire calculation for neutrino oscillation probabilities.

In the framework of standard model extension, we consider the Lagrangian^{41,42} for neutrino sector given by

$$\mathcal{L} = \frac{1}{2} i \bar{\nu}_A \gamma^\mu \overleftrightarrow{\partial}_\mu \nu_B \delta_{AB} + \frac{1}{2} i c_{AB}^{\mu\nu} \bar{\nu}_A \gamma^\mu \overleftrightarrow{\partial}^\nu \nu_B - a_{AB}^\mu \bar{\nu}_A \gamma^\mu \nu_B, \quad (1)$$

where μ, ν are spinor indices and A, B are flavor indices. $c_{AB}^{\mu\nu}$ and a_{AB}^μ are LV parameters. In Eq. (1), the first term is consistent with the minimal standard model; the second and third terms describe the contribution from Lorentz violation, which denote CPT even term and CPT odd term respectively. For the convenience of calculation, we transform the lagrangian as

$$\mathcal{L}' = i \bar{\nu}_A \gamma^\mu \partial_\mu \nu_B \delta_{AB} + i c_{AB}^{\mu\nu} \bar{\nu}_A \gamma^\mu \partial^\nu \nu_B - a_{AB}^\mu \bar{\nu}_A \gamma^\mu \nu_B, \quad (2)$$

where \mathcal{L}' equals to \mathcal{L} in quantum field theory, because divergence terms have no contribution to the action. The Euler-Lagrange equation of motion for neutrinos can be written as

$$i \gamma^0 \partial_0 \nu_A + i \gamma^i \partial_i \nu_A + i c_{AB}^{\mu\nu} \gamma^\mu \partial^\nu \nu_B - a_{AB}^\mu \gamma^\mu \nu_B = 0. \quad (3)$$

A new motion equation can be obtained by multiplying Eq. (3) with the matrix γ^0 . Comparing the new equation with the conventional equations of motion $(i \delta_{AB} \partial_0 - \mathcal{H}_{AB}) \nu_A = 0$, we obtain the Hamiltonian for neutrinos

$$\mathcal{H} = -i \gamma^0 \gamma^i \partial_i - i c_{AB}^{\mu\nu} \gamma^0 \gamma^\mu \partial^\nu + a_{AB}^\mu \gamma^0 \gamma^\mu. \quad (4)$$

Note the unconventional time-derivative term in Eq. (3) has been included in Eq. (4). The above discussion is within the context of quantum field theory. Now we transform the description into quantum mechanics and treat the differential operator as momentum operator to study neutrinos with a fixed momentum. In this paper, we focus on the upper bounds of Lorentz violation contribution to neutrino oscillation and so far right-handed neutrinos or left-handed antineutrinos have not been detected experimentally. So we assume that neutrinos are massless. Our calculation is based on three-generation model. With the basic vector $(u_L(p), v_R(-p))^T$, the Hamiltonian matrix for neutrinos can be given by

$$H_{AB} = \begin{pmatrix} |\vec{p}| \delta_{AB} + c_{AB}^{\mu\nu} \frac{p_\mu p_\nu}{|\vec{p}|} + a_{AB}^\mu \frac{p_\mu}{|\vec{p}|} & 0 \\ 0 & |\vec{p}| \delta_{AB} + c_{AB}^{\mu\nu} \frac{p_\mu p_\nu}{|\vec{p}|} - a_{AB}^\mu \frac{p_\mu}{|\vec{p}|} \end{pmatrix}. \quad (5)$$

Substituting Eq. (5) into Eq. (3) the general dynamical equation for neutrinos could be obtained. Then we can study the dynamical character of neutrinos by calculating the dynamical equation. However, we are more interested in neutrino oscillation probability in this work. So we just need to figure out the eigenenergy for neutrinos by diagonalizing the Hamiltonian. In Eq. (5), the up-diagonal term is the Hamiltonian for left-handed neutrinos and the down-diagonal term is the

Hamiltonian for right-handed antineutrinos. We just study the left-handed neutrino part because the two terms have the similar form. We simplify the Hamiltonian H_{AB} as

$$h_{AB} = |\vec{p}| \delta_{AB} + c_{AB}^{\mu\nu} \frac{p_\mu p_\nu}{|\vec{p}|} + a_{AB}^\mu \frac{p_\mu}{|\vec{p}|}, \quad (6)$$

where $A, B = e, \mu, \tau$. To figure out neutrino eigenenergy we diagonalize the Hamiltonian matrix (6) by a 3×3 matrix U . Note that U is a unitary matrix. The eigenenergy matrix is

$$E_{IJ} = U_{IA}^\dagger h_{AB} U_{BJ}, \quad (7)$$

where E is a diagonalized matrix. The eigenenergy can be labeled as E_I , where $I = 1, 2, 3$. Neutrino energy eigenstates are the linear combination of flavor eigenstates because matrix U is unitary:

$$|\nu_I\rangle = (U^\dagger)_{IA} |\nu_A\rangle, \quad (8)$$

where I and A represent different eigenstates and flavor eigenstates respectively. Because the matrix U is unitary, Eq. (8) can be transformed as

$$|\nu_A(t)\rangle = \sum_{IB} (U^\dagger)_{IA}^* e^{-iE_I t} (U^\dagger)_{IB} |\nu_B\rangle. \quad (9)$$

Neutrinos propagate at the speed of light approximately because we have assumed that neutrinos are massless and that LV parameters is small. When the propagation length is L , the flavor state can be written as

$$|\nu_A(L)\rangle = \sum_{IB} (U^\dagger)_{IA}^* e^{-iE_I L} (U^\dagger)_{IB} |\nu_B\rangle. \quad (10)$$

From Eq. (10) and the unitary of U , the oscillation probability can be expressed as

$$\begin{aligned} P(\nu_A \rightarrow \nu_B) &= \delta_{AB} \\ &- 4 \sum_{I>J} \Re[(U^\dagger)_{IA}^* (U^\dagger)_{IB} (U^\dagger)_{JA}^* (U^\dagger)_{JB}] \sin^2\left(\frac{\Delta E_{IJ}}{2} L\right) \\ &+ 2 \sum_{I>J} \Im[(U^\dagger)_{IA}^* (U^\dagger)_{IB} (U^\dagger)_{JA}^* (U^\dagger)_{JB}] \sin^2(\Delta E_{IJ} L), \end{aligned} \quad (11)$$

where \Re and \Im denote the real and imaginary parts respectively.

3. Specific models and bounds on LV parameters

In Sect. 2, we obtained the analytic equations for neutrino oscillation. In this section, we discuss three specific models. Comparing with the experimental results, we will figure out the upper bounds on LV parameters in different models. The Lorentz non-invariant direction-dependent oscillations for massless neutrinos are not supported by recent research work^{43,44}. So in this part we try to build a massless neutrino

6 *Shimin Yang and Bo-Qiang Ma*

model without direction-dependent oscillations. All the three special models in our work are direction-independent.

In Eq. (6), h_{AB} is a 3×3 matrix in neutrino generation space. To reduce the LV parameters, we assume that the neutrino Hamiltonian can be simplified as

$$h_{AB} = \begin{pmatrix} E & \varepsilon & 0 \\ \varepsilon & E + \eta & \zeta \\ 0 & \zeta & E \end{pmatrix}, \quad (12)$$

where $E = |\vec{p}|$, $\varepsilon = c_{e\mu}^{00} p_0 + a_{e\mu}^0 = c_{e\mu}^{00} E + a_{e\mu}^0$, $\zeta = c_{\mu\tau}^{00} E + a_{\mu\tau}^0$, and $\eta = c_{\mu\mu}^{00} E + a_{\mu\mu}^0$. Lorentz violation parameters are defined in a sun-centered inertial frame. There are 6 non-zero LV parameters in the above specific model, and the other LV parameters are zero.

By substituting Eq. (12) into Eq. (7), the eigenenergy matrix E and mixing matrix U could be figured out as

$$E_{IJ} = \begin{pmatrix} E & 0 & 0 \\ 0 & E + \frac{\eta}{2} - \frac{\sqrt{4\varepsilon^2 + 4\zeta^2 + \eta^2}}{2} & 0 \\ 0 & 0 & E + \frac{\eta}{2} + \frac{\sqrt{4\varepsilon^2 + 4\zeta^2 + \eta^2}}{2} \end{pmatrix}, \quad (13)$$

and

$$U^\dagger = \begin{pmatrix} -\frac{\zeta}{\sqrt{\varepsilon^2 + \zeta^2}} & 0 & \frac{\varepsilon}{\sqrt{\varepsilon^2 + \zeta^2}} \\ \frac{\varepsilon}{\sqrt{N}} & \frac{\eta - \sqrt{4(\varepsilon^2 + \zeta^2) + \eta^2}}{2\sqrt{N}} & \frac{\zeta}{\sqrt{N}} \\ \frac{\varepsilon}{\sqrt{M}} & \frac{\eta + \sqrt{4(\varepsilon^2 + \zeta^2) + \eta^2}}{2\sqrt{M}} & \frac{\zeta}{\sqrt{M}} \end{pmatrix}, \quad (14)$$

where

$$\begin{aligned} M &= 2(\varepsilon^2 + \zeta^2) + \frac{\eta^2}{2} + \frac{\eta\sqrt{4(\varepsilon^2 + \zeta^2) + \eta^2}}{2}, \\ N &= 2(\varepsilon^2 + \zeta^2) + \frac{\eta^2}{2} - \frac{\eta\sqrt{4(\varepsilon^2 + \zeta^2) + \eta^2}}{2}. \end{aligned} \quad (15)$$

With the eigenenergy matrix E and the unitary matrix U , the oscillation probabilities can be expressed as

$$\begin{aligned}
 P(\nu_e \rightarrow \nu_e) &= 1 \\
 &- \frac{4\varepsilon^2\zeta^2}{(\varepsilon^2 + \zeta^2)[\sqrt{2(\varepsilon^2 + \zeta^2) + \frac{\eta^2}{2}} - \frac{\eta\sqrt{4(\varepsilon^2 + \zeta^2) + \eta^2}}{2}]} \sin^2\left[\left(\frac{\eta}{4} - \frac{\sqrt{4\varepsilon^2 + 4\zeta^2 + \eta^2}}{4}\right)L\right] \\
 &- \frac{4\varepsilon^2\zeta^2}{(\varepsilon^2 + \zeta^2)[\sqrt{2(\varepsilon^2 + \zeta^2) + \frac{\eta^2}{2}} + \frac{\eta\sqrt{4(\varepsilon^2 + \zeta^2) + \eta^2}}{2}]} \sin^2\left[\left(\frac{\eta}{4} + \frac{\sqrt{4\varepsilon^2 + 4\zeta^2 + \eta^2}}{4}\right)L\right] \\
 &- \frac{4\varepsilon^4}{(\varepsilon^2 + \zeta^2 + \eta^2)(4(\varepsilon^2 + \zeta^2) + \eta^2)} \sin^2\left[\left(\frac{\sqrt{4(\varepsilon^2 + \zeta^2) + \eta^2}}{2}\right)L\right], \\
 P(\nu_e \rightarrow \nu_\mu) &= \frac{4\varepsilon^2}{4\varepsilon^2 + 4\zeta^2 + \eta^2} \sin^2\left[\left(\frac{\sqrt{4\varepsilon^2 + 4\zeta^2 + \eta^2}}{2}\right)L\right], \\
 P(\nu_\mu \rightarrow \nu_\mu) &= 1 - \frac{4\varepsilon^2 + 4\zeta^2}{4\varepsilon^2 + 4\zeta^2 + \eta^2} \sin^2\left[\left(\frac{\sqrt{4\varepsilon^2 + 4\zeta^2 + \eta^2}}{2}\right)L\right], \\
 P(\nu_\mu \rightarrow \nu_\tau) &= \frac{4\zeta^2}{4\varepsilon^2 + 4\zeta^2 + \eta^2} \sin^2\left[\left(\frac{\sqrt{4\varepsilon^2 + 4\zeta^2 + \eta^2}}{2}\right)L\right], \\
 P(\nu_e \rightarrow \nu_\tau) &= \frac{4\varepsilon^2\zeta^2}{(\varepsilon^2 + \zeta^2)[\sqrt{2(\varepsilon^2 + \zeta^2) + \frac{\eta^2}{2}} - \frac{\eta\sqrt{4(\varepsilon^2 + \zeta^2) + \eta^2}}{2}]} \sin^2\left[\left(\frac{\eta}{4} - \frac{\sqrt{4\varepsilon^2 + 4\zeta^2 + \eta^2}}{4}\right)L\right] \\
 &+ \frac{4\varepsilon^2\zeta^2}{(\varepsilon^2 + \zeta^2)[\sqrt{2(\varepsilon^2 + \zeta^2) + \frac{\eta^2}{2}} + \frac{\eta\sqrt{4(\varepsilon^2 + \zeta^2) + \eta^2}}{2}]} \sin^2\left[\left(\frac{\eta}{4} + \frac{\sqrt{4\varepsilon^2 + 4\zeta^2 + \eta^2}}{4}\right)L\right] \\
 &- \frac{4\varepsilon^2\zeta^2}{(\varepsilon^2 + \zeta^2)(4\varepsilon^2 + 4\zeta^2 + \eta^2)} \sin^2\left[\left(\frac{\sqrt{4\varepsilon^2 + 4\zeta^2 + \eta^2}}{2}\right)L\right], \\
 P(\nu_\tau \rightarrow \nu_\tau) &= 1 \\
 &- \frac{4\varepsilon^2\zeta^2}{(\varepsilon^2 + \zeta^2)[\sqrt{2(\varepsilon^2 + \zeta^2) + \frac{\eta^2}{2}} - \frac{\eta\sqrt{4(\varepsilon^2 + \zeta^2) + \eta^2}}{2}]} \sin^2\left[\left(\frac{\eta}{4} - \frac{\sqrt{4\varepsilon^2 + 4\zeta^2 + \eta^2}}{4}\right)L\right] \\
 &- \frac{4\varepsilon^2\zeta^2}{(\varepsilon^2 + \zeta^2)[\sqrt{2(\varepsilon^2 + \zeta^2) + \frac{\eta^2}{2}} + \frac{\eta\sqrt{4(\varepsilon^2 + \zeta^2) + \eta^2}}{2}]} \sin^2\left[\left(\frac{\eta}{4} + \frac{\sqrt{4\varepsilon^2 + 4\zeta^2 + \eta^2}}{4}\right)L\right] \\
 &- \frac{4\zeta^4}{(\varepsilon^2 + \zeta^2)(4\varepsilon^2 + 4\zeta^2 + \eta^2)} \sin^2\left[\left(\frac{\sqrt{4\varepsilon^2 + 4\zeta^2 + \eta^2}}{2}\right)L\right]. \tag{16}
 \end{aligned}$$

In Eq. (16), oscillation probabilities satisfy the probability unity equation $\sum_B P(\nu_A \rightarrow \nu_B) = 1$, which is guaranteed by the unitarity of U . From above calculation, we can see that not only the eigenenergy splitting ΔE_{ij} but also the mixing parts are functions of LV parameters. To clearly understand the novel effect of Eq. (16), we can analyze $P(\nu_\mu \rightarrow \nu_\tau)$ with a special choice of LV parameters. If η is the only nonzero CPT even LV parameter, then $\eta = c_{\mu\mu}^{00} E$, $\varepsilon = a_{e\mu}^0$, $\zeta = a_{\mu\tau}^0$. Now both the mixing part and the eigenenergy splitting ΔE_{ij} are functions of neutrino

8 *Shimin Yang and Bo-Qiang Ma*

energy. In the conventional massive neutrino model, the corresponding probability can be expressed as $P(\nu_\mu \rightarrow \nu_\tau) = \sin^2 2\theta \cdot \sin^2[1.27 \Delta m^2(L/E)]$, while the mixing part $\sin^2 2\theta$ is independent of energy. So the amplitude of conventional massive neutrino oscillation is fixed, and the phenomenon of oscillation disappears when the neutrino energy is high enough because the oscillation P directs to L/E at high energy. But in Eq. (16), we can clearly see that the mixing part of $P(\nu_\mu \rightarrow \nu_\tau)$ is a function of neutrino energy. So oscillation amplitude varies with neutrino energy. By further calculation, as shown in 3.1, the oscillation probability will be suppressed at high energy, which is consistent with the conventional massive model, but the suppressed threshold energy is much higher comparing with the conventional massive model.

There would be different novel behaviors of the neutrino oscillation in the presence of Lorentz violation by choosing different LV parameters. In the following we will study three special cases with different kinds of choosing LV parameters. By comparing with the exiting experimental data, we can constrain LV parameters.

3.1. Model 1 Non-diagonal terms are CPT-Odd parameters with CPT-Even parameters only in the diagonal term

If we assume that $a_{e\mu}^0$, $a_{\mu\tau}^0$, and $c_{\mu\mu}^{00}E$ are nonzero, then

$$\varepsilon = a_{e\mu}^0, \quad \zeta = a_{\mu\tau}^0, \quad \eta = c_{\mu\mu}^{00}E. \quad (17)$$

Substitute these LV parameters into Eq. (11). To calculate the numerical results of LV parameter, we compare the theoretical equations with experimental results.

KamLAND detected $P(\nu_e \rightarrow \nu_e) \simeq 61\%$ with neutrino energy $E \simeq 4.3$ MeV and neutrino propagation length $L \simeq 180$ km⁴⁵. MINOS observed muon neutrino disappearance with neutrino energy $E \simeq 4.9$ GeV and propagation length $L \simeq 735$ km, $P(\nu_\mu \rightarrow \nu_\mu) \simeq 76\%$ ⁴⁶. We also get the flavor change channel of muon neutrino to tau neutrino from K2K, $P(\nu_\mu \rightarrow \nu_\tau) \simeq 36\%$ with $E \simeq 1.8$ GeV, $L \simeq 250$ km⁴⁷.

Substituting these experimental data into Eq. (11), we get three equations with three LV parameters. Because this is a nonlinear system of equations, the solution is not unique. But we can give the order of LV parameters in principle: $a_{e\mu}^0 \sim a_{\mu\tau}^0 \sim 10^{-11}$ eV and $c_{\mu\mu}^{00} \sim 10^{-20}$.

For further restriction of LV parameters, we use the experimental results for the oscillation channel of electron neutrino to muon neutrino. LSND has used muon sources from the decay $\pi^+ \rightarrow \mu^+ + \nu_\mu$ to detect neutrino oscillation in the subsequent decay of the muon through $\mu^+ \rightarrow e^+ + \nu_e + \bar{\nu}_\mu$ ⁴⁸. This experiment finds the oscillation $\bar{\nu}_\mu \rightarrow \bar{\nu}_e$ (with $20 \text{ MeV} \leq E_{\nu_\mu} \leq 58.2 \text{ MeV}$) with a probability of 0.26%. However, the MiniBoone experiment, which was expected to verify the results of LSND, has reported their first result which does not favor the simple explanation of the LSND results based on the two flavor neutrino oscillation⁴⁹. In this paper, we use the experimental results from K2K about the oscillation channel $\nu_\mu \rightarrow \nu_e$ with the mixing angle $\sin^2 2\theta_{\mu e} < 0.13$ ⁵⁰. Now we plot the oscillation probability

as a function of the neutrino energy E , and as a function of the path length L , respectively, with the LV parameters $a_{e\mu}^0 = 1.09 \times 10^{-11}$ eV, $a_{\mu\tau}^0 = 2.97 \times 10^{-11}$ eV, and $c_{\mu\mu}^{00} = 1.42 \times 10^{-20}$.

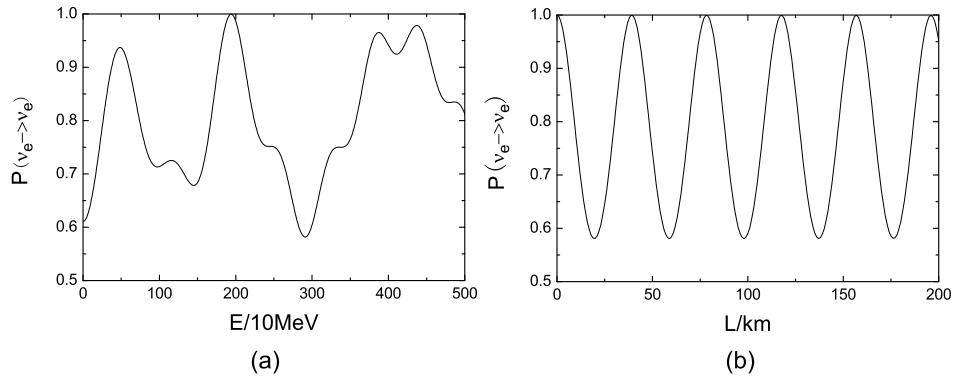


Fig. 1. Neutrino oscillation probabilities for $\nu_e \rightarrow \nu_e$. (a) The left plot shows the oscillation probability as a function of neutrino energy with a fixed path length $L = 180$ km. (b) The right plot shows the oscillation probability as a function of path length with a fixed energy $E = 10$ MeV.

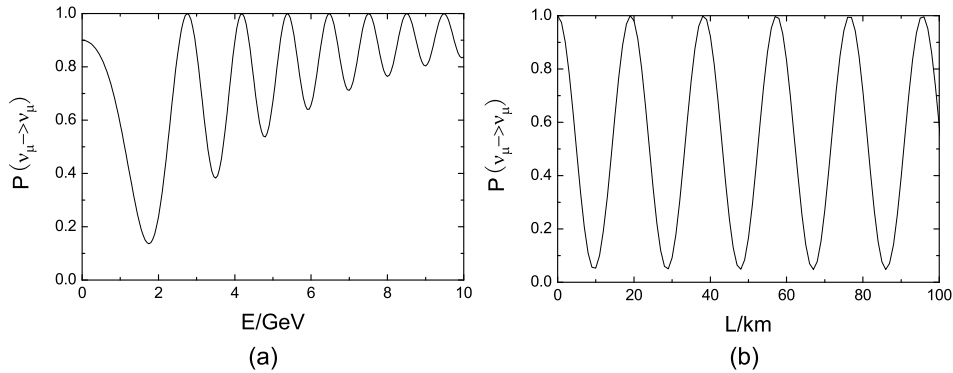


Fig. 2. Neutrino oscillation probabilities for $\nu_\mu \rightarrow \nu_\mu$. (a) The left plot shows the oscillation probability as a function of neutrino energy with a fixed path length $L = 100$ km. (b) The right plot shows the oscillation probability as a function of path length with a fixed energy $E = 1$ GeV.

Fig. 1 shows the oscillation probability for $\nu_e \rightarrow \nu_e$ as a function of the neutrino energy E with a fixed path length $L = 180$ km, and as a function of the propagation length L with neutrino energy $E = 10$ MeV, respectively. Comparing with the results of massive neutrino scenario, we find that in Lorentz violation model electron neutrino does not have drastic oscillation at low energy. This is different from the conventional massive neutrino scenario. In conventional neutrino model, the phenomena of neutrino oscillation ($\nu_e \rightarrow \nu_e$) disappears at high energy ($E > 100$ MeV

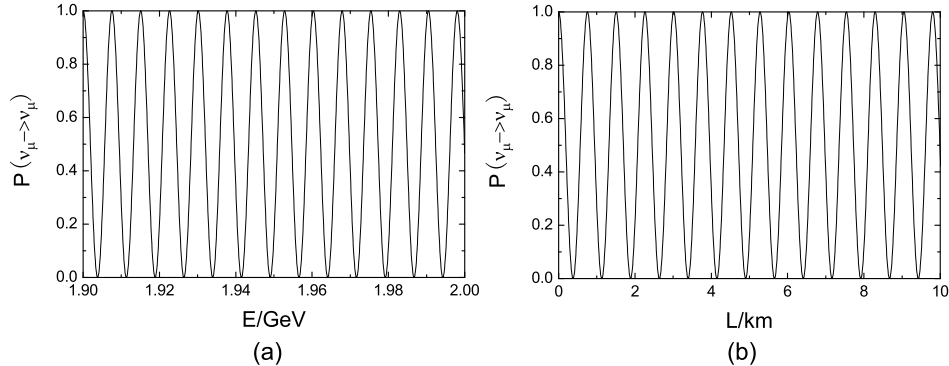
10 *Shimin Yang and Bo-Qiang Ma*

Fig. 3. Neutrino oscillation probabilities for $\nu_\mu \rightarrow \nu_\mu$. (a) The left plot shows the oscillation probability as a function of neutrino energy with a fixed path length $L = 100$ km. (b) The right plot shows the oscillation probability as a function of path length with a fixed energy $E = 1$ GeV.

with a fixed path length $L = 180$ km). However, in Fig. 1 we find the existence of oscillations at high energy. This distinction is resulted from different dependence on neutrino energy for oscillation probability. In addition, the mixing part is fixed in convention massive model. But in Fig. 2 we could find that the neutrino oscillation amplitude varies with neutrino energy. These novel effects can be tested at high energy sector. Because the dependence on path length has the same form in two different models (massive neutrino model and Lorentz violation model), the plots of path length dependence have no remarkable distinction with the conventional massive neutrino model.

3.2. Model 2 non-diagonal terms are CPT-Even parameters with CPT-Odd parameters only in the diagonal term

If we assume that $a_{\mu\mu}^0$, $c_{e\mu}^{00}$, and $c_{\mu\tau}^{00}$ are nonzero, then

$$\varepsilon = c_{e\mu}^{00} E, \quad \zeta = c_{\mu\tau}^{00} E, \quad \eta = a_{\mu\mu}^0. \quad (18)$$

Substitute these LV parameters into Eq. (11). Similarly to Model 1, we use KamLAND, K2K and MINOS experimental results to compute the parameters. The numerical values are also consistent with experimental results about the oscillation channel $\nu_\mu \rightarrow \nu_e$ from K2K. Fig. 3 shows the oscillation probability of the channel $\nu_\mu \rightarrow \nu_\mu$ as a function of the neutrino energy E and as a function of the propagation length L respectively with LV parameters $a_{\mu\mu}^0 = 1.58 \times 10^{-12}$ eV, $c_{e\mu}^{00} = 2.93 \times 10^{-19}$, and $c_{\mu\tau}^{00} = 7.68 \times 10^{-19}$.

The order of LV parameters c_{AB} is larger than that of Model 1, so the oscillation periods of the changing probabilities against neutrino energy and path length are much smaller than those in Model 1. In addition, the oscillation amplitude is steady at high energy, which is different comparing with Model 1. When neutrino energy is high enough, parameters ε and ζ are much larger than η because ε and ζ

linearly depend on neutrino energy. LV parameters $c_{e\mu}^{00}$ and $c_{\mu\tau}^{00}$ in the numerator and denominator have the same power in the mixing part, so the values of mixing part are steady at high energy.

3.3. Model 3 Both of CPT-Even and CPT-Odd parameters are included in the diagonal term

If we assume that $a_{e\mu}^0$, $a_{\mu\mu}^0$, $a_{\mu\tau}^0$, and $c_{\mu\mu}^{00}$ are nonzero, then

$$\varepsilon = a_{e\mu}^0, \quad \zeta = a_{\mu\tau}^0, \quad \eta = a_{\mu\mu}^0 + c_{\mu\mu}^{00}E. \quad (19)$$

We introduce a new equation $\zeta = x\varepsilon$, then the constraint of the mixing part $\sin^2 2\theta_{\mu e} < 0.13$ from K2K experimental results can be easily satisfied by adjusting the constant x . In our calculation we choose $x = 2.7$. Substitute all these new parameters to Eq. (11). Comparing with KamLAND, K2K and MINOS experimental results, we can figure out the LV parameters. Figs. 4 and 5 show the oscillation probability against neutrino energy E and propagation length L respectively with LV parameters $a_{e\nu}^0 = 1.28 \times 10^{-11}$ eV, $a_{\mu\mu}^0 = 3.40 \times 10^{-11}$ eV, and $c_{\mu\mu}^{00} = 1.04 \times 10^{-20}$.

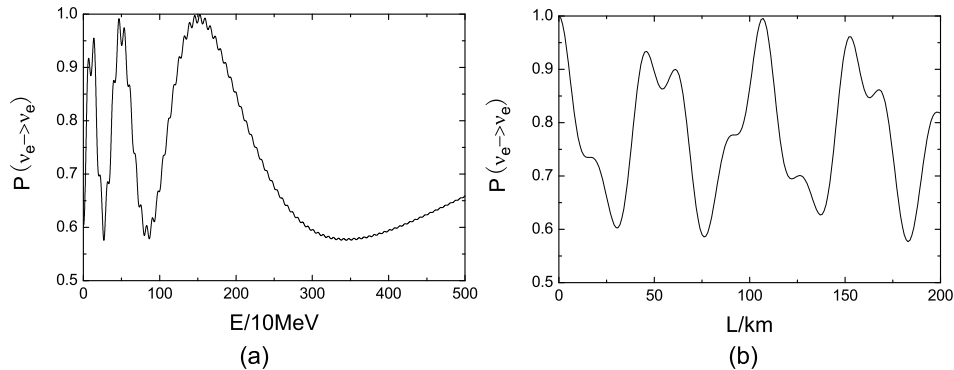


Fig. 4. Neutrino oscillation probabilities for $\nu_e \rightarrow \nu_e$. (a) The left plot shows the oscillation probability as a function of neutrino energy with a fixed path length $L = 180$ km. (b) The right plot shows the oscillation probability as a function of path length with a fixed energy $E = 10$ MeV.

Figs. 4 and 5 keep the main characteristics of Figs. 1 and 2. Neutrinos do not have drastic oscillation at low energy and the oscillation phenomena still exists at high energy, which is different from the massive neutrino scenario. Similar to Model 1, the oscillation amplitude varies in different energy scale. These similarities can be explained by the fact that the oscillation probability dependence on LV parameters and neutrino energy have similar form in the two models .

During the above calculation the boost effect has not been considered. In this work we assumed that the LV parameters are direction independent in the sun-centered frame. The experiments are done on the Earth which is moving around the

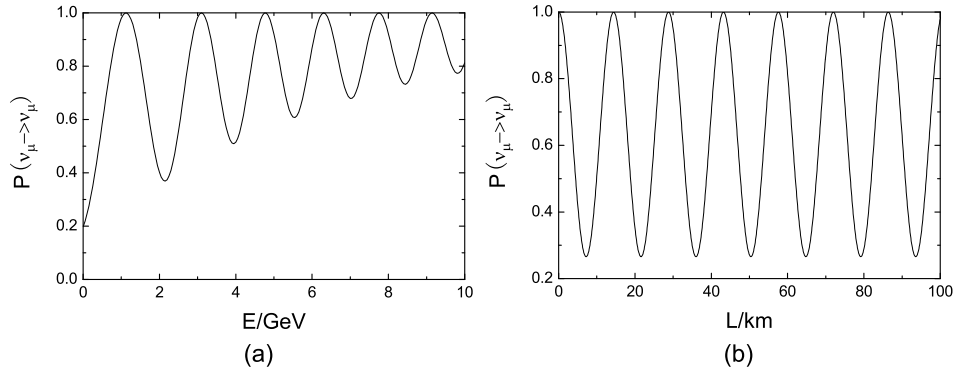


Fig. 5. Neutrino oscillation probabilities for $\nu_\mu \rightarrow \nu_\mu$. (a) The left plot shows the oscillation probability as a function of neutrino energy with a fixed path length $L = 100$ km. (b) The right plot shows the oscillation probability as a function of path length with a fixed energy $E = 1$ GeV.

sun and is also rotating. The experiments in laboratories therefore see LV parameters which have direction dependence because there is a boost. When the long baseline experiments based on the earth are discussed, the boost effect would cause some influence on the direction dependent parameters. As the earth moving velocity is much smaller than the light speed, the boost effect, which is about 10^{-4} for orbit and 10^{-6} for rotation respectively, leads to little impact to the numerical values of the direction independent parameters (a^0 and c^{00}) in the earth inertial frame. But the influence on the direction dependent parameters a^x and c^{0x} , which are about 10^{-4} order comparing to the corresponding direction independent parameters, needs to be compared with the upper bounds given in Ref. 51. In our model 2, the direction dependent parameter c^{0x} induced by boost effect has the same order comparing with the upper bound in Ref. 51. Further constraints from future experiments for direction dependent parameters would be a challenge for this model. Therefore Ref. 51 has put a strict constraint for the sun-centered directional independent models built in this work. However, a model with smaller direction independent parameters, such as our model 1 and model 3, is consistent with the experimental data.

In addition, LSND data are not used during the calculation of the three different kinds of models. Substituting the LV parameters numerical results of these models into the equation $P(\bar{\nu}_\mu \rightarrow \bar{\nu}_e)$ respectively, we find that the oscillation probability are much smaller than the oscillation probability of $(0.26 \pm 0.067 \pm 0.045)\%$ reported by LSND. So in our work the explanation of the LSND data based on the two flavor neutrino oscillation is unfavored. While in this work we assume that only a limited special number of LV parameters are nonzero, there are still large freedoms to fit experimental results with Lorentz violation models, e.g., Ref. 36 explained all class of experimental data, including LSND, with a massive Lorentz violation model. How to explain LSND data would need more experimental and theoretical work.

4. Conclusion

In this paper, we calculated Lorentz violation (LV) contribution to neutrino oscillation by the effective field theory for LV (Standard Model Extension). We assume that neutrinos are massless and that there are only three generations of left-hand neutrinos and right-handed antineutrinos in nature. Unlike the conventional massive neutrino scenario, in our calculation neutrino flavor states are not the mixing states of neutrino mass eigenstates but neutrino energy eigenstates. In this work, the equation of neutrino oscillation probabilities given by Eq. (11) is a complete analytic equation and contains hundreds of LV parameters. In section 3, we introduced three direction-independent specific models. Comparing with neutrino experimental results, the upper bounds on LV parameters can be figured out. We have checked our calculation results with the experimental results in Ref. 51. In model 2, the directional dependent parameters c_{0x} induced by the boost effect are smaller than the upper bounds given in Ref. 51 but with the same order. And slightly mediations for the directional independent parameters in model 2 may lead to its failure. So Ref. 51 has put a strict constraints for the sun-centered directional independent models built in this work. And a model with smaller directional independent parameters, such as model 1 and model 3, is much better to accord with the experimental data. From Figs. 1–5 we see that neutrinos do not have drastic oscillations at low energy and oscillations still exist at high energy. Furthermore, the oscillation amplitude varies with the neutrino energy. All these characteristics are different from the massive neutrino scenario. In addition, the three models in this paper have different characteristics, too. The main difference lays in the relationship between oscillation probabilities and neutrino energy. In models 1 and 3, the oscillation amplitude varies in different energy scale and goes to zero when the neutrino energy is high enough. But in model 2, the oscillation amplitude is steady at high energy. These different models can be tested and constrained in high energy neutrino experiments.

We also aware the negative report for Lorentz violation from existing atmospheric neutrino data. Refs.^{52,53,54} presented detailed analysis of the zenith angle distribution of atmospheric neutrino events from Super-Kamiokande underground experiment. The analysis of super-Kamiokande data disfavors Lorentz-invariance as the leading source of atmospheric neutrino oscillation. There are several potential reasons to explain this difficulty. First, Lorentz violation is not the leading mechanism for atmosphere neutrinos and the contribution of massive mechanism to neutrino oscillation can not be neglected at this range. From another point of view, in our calculation the mixing part is a function of neutrino energy and as Fig. 2 shown, the oscillation amplitudes are suppressed at high energy, which is different from the Lorentz violation model used in Refs.^{52,53,54}. (The effect of oscillation suppressing at high neutrino is general consistent with the conventional massive model, though the suppressed threshold energy is different between the two kinds of mechanisms). So these novel effects in our model would produce some new effect in analyzing atmosphere neutrino from the view of Lorentz violation.

In the above discussion, we assume that neutrinos are massless and that Lorentz violation is the only origin of neutrino oscillation. So we can clearly see what kind of new effect will occur if Lorentz violation exists in neutrino sector. It is possible that neutrinos have small mass and both Lorentz violation and the conventional oscillation mechanism contribute to neutrino oscillation. Then LV parameter will be further constrained and our numerical calculation for LV parameters could only be considered as an upper bound for LV. It is difficult to distinguish between these two kinds of mechanism at low energy. But high energy experiment is a good avenue to test Lorentz violation models. In the conventional massive model, the mixing part is independent of energy and neutrino oscillations disappear at high energy because the oscillation P is proportional to L/E . But in Lorentz violation models, mixing part is the function of energy and the oscillation amplitude varies with neutrino energy. Thus neutrino experiments with energy dependence may distinguish between the conventional massive neutrino scenario and the Lorentz violation scenario for neutrino oscillations.

Acknowledgments

We acknowledge Zhi-Qiang Guo, Shi-Wen Li, and Zhi Xiao for useful discussions. This work is partially supported by National Natural Science Foundation of China (Nos. 10721063, 10575003, 10528510), by the Key Grant Project of Chinese Ministry of Education (No. 305001), by the Research Fund for the Doctoral Program of Higher Education (China).

References

1. V. A. Kostelecký and S. Samuel, *Phys. Rev. D* **39**, 683 (1989).
2. J. R. Ellis, N. E. Mavroumatos and D. V. Nanopoulos, gr-qc/9909085; O. Bertolami, R. Lehnert, R. Potting and A. Ribeiro, *Phys. Rev. D* **69**, 083513 (2004).
3. C. P. Burgess, J. Cline, E. Filotas, J. Matias and G. D. Moore, *J. High Energy Phys.* **03**, 043 (2002).
4. R. Gambini and J. Pullin, *Phys. Rev. D* **59**, 124021 (1999).
5. M. R. Douglas and N. A. Nekrasov, *Rev. Mod. Phys.* **73**, 977 (2001).
6. S. Chadha and H. B. Nielsen, *Nucl. phys. B* **217**, 125 (1983).
7. P. Kraus and E. T. Tomboulis, *Phys. Rev. D* **66**, 045015 (2002).
8. A. Jenkins, *Phys. Rev. D* **69**, 105007 (2004).
9. T. Damour and A. M. Polyakov, *Nucl. phys. B* **423**, 532 (1994).
10. N. Arkani-Hamed, H. C. Cheng, M. A. Luty and S. Mukohyama, *J. High Energy Phys.* **05**, 074 (2004).
11. V. A. Kostelecký, R. Lehnert and M. J. Perry, *Phys. Rev. D* **68**, 123511 (2003).
12. O. Bertolami, R. Lehnert, R. Potting and A. Ribeiro, *Phys. Rev. D* **69**, 083513 (2004).
13. J. W. Moffat, *Int. J. Mod. Phys. D* **2**, 351 (1993).
14. J. Magueijo, *Rept. Prog. Phys.* **66**, 2025 (2003).
15. S. R. Coleman and S.L. Glashow, hep-ph/9808446.
16. S.R. Coleman and S.L. Glashow, *Phys. Rev. D* **59**, 116008 (1999).
17. T. Kifune, *Astrophys. J. Lett.* **L21**, 518 (1999).

18. R.J. Protheroe and H. Meyer, *Phys. Lett. B* **493**, 1 (2000).
19. G. Amelino-Camelia and T. Piran, *Phys. Lett. B* **497**, 265 (2001).
20. Wolfgang Bietenholz, arXiv:0806.3713v2.
21. HEGRA Collab. (F. Aharonian *et al.*), *Astron. Astrophys.* **349**, 29 (1999).
22. K. Greisen, *Phys. Rev. Lett.* **16**, 748 (1966).
23. G. T. Zatsepin and V. A. Kuzmin, *JETP Lett.* **4**, 78 (1966).
24. M. Takeda *et al.*, *Phys. Rev. Lett.* **81**, 1163 (1998).
25. Z. Xiao, B.-Q. Ma, *Int. J. Mod. Phys. A* **24**, 1359 (2009).
26. High Resolution Flys Eye Collab. (R. Abbasi *et al.*), *Phys. Rev. Lett.* **100**, 101101 (2008).
27. Pierre Auger Collab. (J. Abraham *et al.*), *Science* **318**, 938 (2007);
The Pierre Auger Collab. (J. Abraham *et al.*), *Phys. Rev. Lett.* **101**, 061101 (2008).
28. D. Mattingly, *Living Rev. Rel.* **8**, 5 (2005).
29. M. Mewes, hep-ph/0409344.
30. Z. Maki, M. Nakagawa and S. Sakata, *Prog. Theor. Phys.* **28**, 870 (1962).
31. B. Pontecorvo, *Zh. Eksp. Teor. Fiz.* **33**, 549 (1957).
32. S. R. Coleman and S. L. Glashow, *Phys. Lett. B* **405**, 249 (1997).
33. V. Barger, S. Pakvasa, T. J. Weiler and K. Whisnant, *Phys. Rev. Lett.* **85**, 5055 (2000).
34. V. A. Kostelecký and M. Mewes, *Phys. Rev. D* **69**, 016005 (2004).
35. V. A. Kostelecký and M. Mewes, *Phys. Rev. D* **70**, 031902 (2004).
36. T. Katori, V. A. Kostelecký and R. Tayloe, *Phys. Rev. D* **74**, 105009 (2006).
37. Y. Grossman, C. Kilic, J. Thaler and G. E. Walker, *Phys. Rev. D* **72**, 125001 (2005).
38. P. Arias, J. Gamboa, F. Méndez, A. Das and J. Lopez-Sarión, *Phys. Lett. B* **650**, 401 (2007).
39. D. Morgan, E. Winstanley, J. Bruuner and L. F. Thompson, arXiv:0705.1897.
40. D. Colladay, V. A. Kostelecký, *Phys. Rev. D* **55**, 6760 (1997).
41. D. Colladay, V. A. Kostelecký, *Phys. Rev. D* **58**, 116002 (1998).
42. V. A. Kostelecký, R. Lehnert, *Phys. Rev. D* **63**, 065008 (2001).
43. V. Barger, D. Marfatia, K. Whisnant *Phys.Lett.B* **653**, 267 (2007).
44. MINOS Collab. (P. Adamson *et al.*), *Phys. Rev. Lett.* **101**, 151601 (2008).
45. KamLAND Collab. (K. Eguchi *et al.*), *Phys. Rev. Lett.* **90**, 021802 (2003);
KamLAND Collab. (K. Eguchi *et al.*), *Phys. Rev. Lett.* **94**, 081801 (2003).
46. MINOS Collab. (D. G. Michael *et al.*), *Phys. Rev. Lett.* **97**, 191801 (2006).
47. K2K Collab. (E. Aliu *et al.*), *Phys. Rev. Lett.* **94**, 081802 (2005).
48. LSND Collab. (A. Aguilar *et al.*), *Phys. Rev. D* **64**, 112007 (2001);
LSND Collab. (C. Athanassopoulos *et al.*), *Phys. Rev. Lett.* **81**, 1774 (1998).
49. MiniBooNE Collab. (A. A. Aguilar-Arevalo *et al.*), *Phys. Rev. Lett.* **98**, 231801 (2007).
50. K2K Collab. (S. Yamamota *et al.*), *Phys. Rev. Lett.* **96**, 181801 (2006).
51. V. A. Kostelecký, N. Russell, arXiv:0801.0287
52. P. Lipari and M. Lusignoli, *Phys. Rev. D* **60**, 013003 (1999).
53. G. L. Fogli, E. Lisi, A. Marrone and G. Scioscia, *Phys. Rev. D* **60**, 053006 (1999).
54. M. C. Gonzalez-Garcia and M. Maltoni, *Phys. Rev. D* **70**, 033010 (2004).